SOME APPROACHES TO SHAPE ANALYSIS

Anuj Srivastava *Washington Mio*

Department of Statistics Department of Mathematics
anuj@stat.fsu.edu *mio@math.fsu.edu*
Florida State University
Tallahassee, FL 32306, USA

ABSTRACT

Analysis of shapes is important for image analysis. The notion of shapes has been used in a variety of ways across the literature. From the definition of a shape, to the derivation of statistical procedures for shape analysis, the usage of shape is different among different papers. In this paper, we summarize common attributes of different approaches, and compare a few commonly used ones. In particular, we focus on a landmark-based shape analysis, a diffeomorphism approach to shape matching, and a geometric approach to analyzing shapes of curves.

1. INTRODUCTION

Detection, extraction and recognition of objects images is an important area of research. Objects can be characterized using a variety of features: edges, boundaries, colors, motion, shapes, locations etc. These features are often used in a statistical framework to perform image analysis. In other words, one defines a feature space, learns probability models on these spaces using past (training) data, and uses them to conduct statistical inferences in future applications. Shape is a key feature of imaged objects and often provides a reliable way of studying objects as they appear images. Tools for shape analysis can prove important in several applications including medical image analysis, face recognition, fingerprint analysis, space exploration, and underwater search.

One reason for pursuing shape analysis is the possibility that an efficient representation and analysis of shapes can help even in situations where the observations are corrupted, e.g. when images have excess clutter or partial obscuration. Shape is a global feature that can help overcome loss of local data that results from partial obscuration, or from structure less clutter. This possibility, along with the development of statistical methods, has led to the idea of Bayesian shape analysis. In this approach, contextual knowledge is used to impose prior probabilities on shape spaces, followed by the use of posterior probabilities to perform inferences.

In this paper, we review some current techniques used for statistically analyzing shapes of objects in images. Although there is a multitude of approaches described in the literature, we focus here only on a few broad ideas. Our goal is to point out the common elements amongst these approaches, and to compare them by highlighting their differences.

This paper is organized as follows: In section 2, we first present a discussion of general ideas common to various approaches. In Section 3, we look at a few individual approaches to shape analysis and analyze their similarities and differences. We conclude the paper in Section 4 with a brief summary.

2. GENERAL SHAPE ANALYSIS

In this section, we summarize elements of shape analysis common to most approaches.

2.1 Shape Representations

Although a number of researchers have utilized the notion of shapes in image analysis, there is no universal agreement on its definition and usage. The breadth and scope of applications may require that the analysis be adapted to the specific task at hand. These treatments even differ in what is considered a part of shape of an object. Some descriptions are restricted only to the boundaries of objects. Here, one analyzes the contour curves for 2D objects or boundary surfaces of 3D objects, for example as shown in the middle row of Figure 1. Other papers consider both the boundaries and the interior regions of objects in shape analysis. A large body of work in shape analysis considers shape as identified by a number of landmark points on the object (either on the boundary or in interior), as shown in the bottom row. Some researchers include the object textures, given by pixels values in images, while others ignore textures and focus only on the locations (coordinates of points of interest).

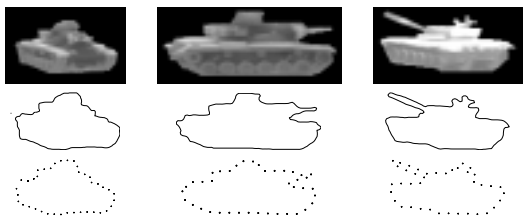

Figure 1: Different representations of shapes. Some researchers use full images, shown in the top row, in a shape analysis, while others restrict to boundary curves, shown in the middle row, for that purpose. Some others use only the landmark points with examples shown in the bottom row.

We will use $\mathscr{C}$ to denote the set of all values attained by these shape descriptors. Later, we will make it precise in the context of different approaches.

2.2 Shape as an Equivalence Class

Despite differences in the definition and usage of shapes, certain attributes have been consistently associated with shapes across the literature. For instance, shape is a property that is considered invariant to rigid transformations such as rotations and translations. Also, a uniform scaling of object coordinates is viewed as preserving its shape. Thus, rigid

rotations, translations, and uniform scaling are termed as *shape preserving* transformations or *similarity* transformations. Shown in Figure 2 is an example of the same shape rendered at different similarity transformations.

The set of all possible similarity transformations, call it T, forms a *group*. A group is a set endowed with an associative operation (denoted here by $\circ$) with the property that there is an identity element *id*, and every element has an inverse. (please refer to [16] for more details). The group structure is instrumental in structuring compositions of the transformations: one transformation (t_1) applied after another transformation (t_2) have an equivalent effect of a third transformation (t_3) applied alone. The third transformation is a product of the first two, $t_3 = t_2 \circ t_1$. For example, the set of all orthogonal matrices with determinant $+1$, denoted by $SO(n)$, forms the rotation group, and $\mathbb{R}^n$ forms the translation group. Together, they form the group of rigid motion $SE(n) \equiv SO(n) \ltimes \mathbb{R}^n$; $\mathbb{R}_+$ forms the scale group. Let $T \equiv (SE(n) \times \mathbb{R}_+)$ denote the group of similarity transformations and let $s \in \mathscr{C}$ be a representation of a shape. For a $\tau \in \mathbb{R}^n$, $O \in SO(n)$, and $\rho \in \mathbb{R}_+$, their action on a point $p \subset \mathbb{R}^n$ is given by

$$p \mapsto (Op\rho + \tau) .$$

For $s \in \mathscr{C}$, the action of t on s, denoted by $t \cdot s$, implies the action of t on each element of s. Then,

$$T \cdot s = \{t \cdot s | t \in T\} \subset \mathscr{C},$$

denotes the equivalence class of representations containing s. The subset $T \cdot s$ is also called the *orbit* of s under T.

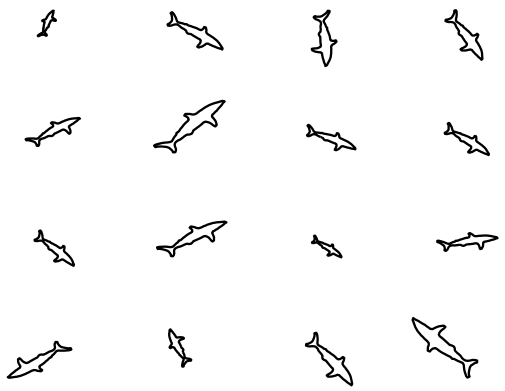

Figure 2: Equivalence of shapes despite different pose and scales.

Despite different components included in description of shapes, eventual shape representations always belong to a quotient space. The shape space is given by $\mathscr{S} \equiv \mathscr{C}/T$, the space obtained by identifying elements that differ from each other by similarity transformations. It is often the case that $\mathscr{C}$ is a Riemannian manifold and its geometry can be used to study the shape space $\mathscr{S}$. Figure 3 shows a cartoon view of $\mathscr{C}$ where each vertical broken line denotes an orbit, or an equivalence class of shapes. Each point on this line can be mapped to any other point on the line by applying an appropriate similarity transformation. Two observed shapes lie on two different vertical lines, if they are indeed different shapes.

2.3 Shape Metrics

An important tool in shape analysis is a metric for quantifying shape dissimilarities. Intrinsic metrics on shape spaces can be obtained using geodesics, which can be loosely defined as shortest paths between given points. The technical definition of a geodesic in $\mathscr{C}$ is slightly different. A path in $\mathscr{C}$ is a geodesic if the covariant derivative of its velocity field vanishes at every point, that is, the intrinsic acceleration of the path is zero. Details on the computation of geodesics will be provided later.

For any $s \in \mathscr{C}$, let $T_s(\mathscr{C})$ denote the space of vectors tangent to $\mathscr{C}$ at s. For a vector $v \in T_s(\mathscr{C})$, there is a unique geodesic $\tilde{\psi}_x(s;v)$ (x denotes the time parameter) starting at s with initial velocity v, that is, $\tilde{\psi}_0(s;v) = s$ and $\dot{\tilde{\psi}}_0(s;v) = v$. v is called the *infinitesimal generator* or simply *generator* of $\tilde{\psi}$. Given $s_1, s_2 \in \mathscr{C}$, one wishes to find a geodesic path connecting them. One can phrase this question as a *shooting problem* in $\mathscr{C}$: find the direction $v \in T_{s_1}(C)$ such that the geodesic starting from s_1 in the direction v reaches the point s_2 in unit time, i.e., $\tilde{\psi}_1(s_1;v) = s_2$. Although in some simple cases, solutions can be found analytically, a numerical approach is adopted in general. The idea is to define a cost function $E(v)$ that is minimized at the desired direction v and treat the construction of geodesics as an optimization problem on the (linear) space $T_{s_1}(\mathscr{C})$.

A metric on the quotient space $\mathscr{S}$ can be defined as follows. If $s_1, s_2 \in \mathscr{C}$ represent shapes in $\mathscr{S}$, let $[s_1], [s_2]$ denote their shape class in $\mathscr{S}$. The distance $d([s_1],[s_2])$ (or simply $d(s_1,s_2)$, abusing notation) is the length of the shortest geodesic in $\mathscr{C}$ from a point in the orbit of s_1 to a point in the orbit of s_2. A geodesic in $\mathscr{C}$ realizing such distance in $\mathscr{S}$ is referred to as a *geodesic* in $\mathscr{S}$.

If T acts on $\mathscr{C}$ by isometries (i.e., without distorting the geometry of $\mathscr{C}$), it can be shown that a geodesic in $\mathscr{C}$ is also a geodesic in the quotient space $\mathscr{S}$, provided that it is perpendicular to the orbits of T it intersects. In addition, a geodesic in C that is perpendicular to one of the orbits is perpendicular to all orbits it meets. Thus, we denote the subspace of $T_s(\mathscr{C})$ formed by all vectors orthogonal to the orbit of s by $T_s(\mathscr{S})$ and call it the tangent space to $\mathscr{S}$ at s. In Figure 3, equivalence classes of shapes are depicted with vertical dashed lines, while geodesics in $\mathscr{S}$ are depicted with horizontal lines.

Given two points $s_1, s_2 \in \mathscr{S}$, we let ψ_x, $0 \leq x \leq 1$, be a geodesic path in $\mathscr{S}$ such that $\psi_0 = s_1$ and $\psi_1 = s_2$ and its length by $d(s_1,s_2)$. Similarly, a geodesic in $\mathscr{S}$ starting at s with initial velocity v will be denoted $\psi_x(s;v)$. The map $\exp\colon T_s(\mathscr{S}) \to \mathscr{S}$ given by $v \mapsto \psi_1(s;v)$ is known as the *exponential map* at s.

2.4 Shape Statistics

The computation of geodesic paths in a shape space is useful for several reasons. In addition to defining a shape metric, it also leads to a notion of mean shape as follows. For a collection of shapes $s_1, s_2, \ldots, s_m \in \mathscr{S}$, a mean is defined as:

$$\mu = \underset{s \in \mathscr{S}}{\operatorname{argmin}} \sum_{i=1}^{m} d(s,s_i)^2 ,$$

where $d(s,s_i)$ is the length of the geodesic connecting s and s_i in $\mathscr{S}$. μ is also known as an intrinsic mean [2], a Karcher mean [8] or a centroid of a distribution. How to find μ? A

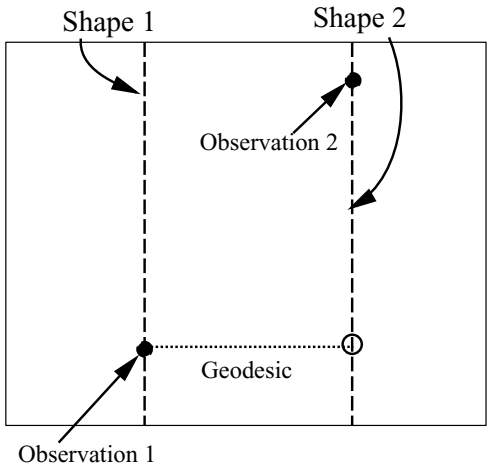

Figure 3: A pictorial illustration of a shape space as a quotient space of $\mathscr{C}$. A geodesic in $\mathscr{C}$ that is perpendicular to the equivalence classes (vertical lines) is also a geodesic in $\mathscr{S}$, denoted by a broken horizontal line here.

gradient-based iterative search for μ is conducted as follows: Let y be a current estimate of μ.

Algorithm 1 *1. Find the geodesic paths $\psi^i(y,s_i)$ from y to s_i, for $i = 1,2,\ldots,m$.*

2. *Compute their direction vectors or generators $v_i = \dot{\psi}_0^i \in T_y(\mathscr{S})$ and compute the average $\bar{v} = \frac{1}{m}\sum_{i=1}^m v_i$.*
3. *Update y by flowing along a geodesic from y in the direction $-2v_m$ for unit time. That is, set $y = \psi_1(y;-2v_m)$.*
4. *Repeat till $\bar{v} = 0$.*

Once a mean shape is computed, the remaining probabilistic formulation follows. Let $T_\mu(\mathscr{S})$ be the space of vectors tangent to the manifold $\mathscr{S}$ at μ. Although $\mathscr{S}$ is a curved space, $T_\mu(\mathscr{S})$ is a vector space of same dimension as $\mathscr{S}$. An exponential map takes elements of $T_\mu(\mathscr{S})$ to $\mathscr{S}$ as follows: for any $v \in T_\mu(\mathscr{S})$, define $\exp_\mu(v) = \psi_1(\mu;v)$, where ψ is the geodesic starting from μ in the direction v. For elements of $\mathscr{S}$ that are close to μ, $\exp_\mu^{-1}$ is well defined, and often easily computed. The linearity of $T_\mu(\mathscr{S})$ helps define a probability distribution on $\mathscr{S}$. First impose a probability density function $f(v)$ on $T_\mu(\mathscr{S})$, and then project it on $\mathscr{S}$ through the exponential map.

In particular, a second order statistic for a collection of shapes can be described as follows. For a given collection $s_1,s_2,\ldots,s_m \in \mathscr{S}$ of shapes, let $\mu \in \mathscr{S}$ be their mean as defined above. Then, for each s_i, let $v_i \in T_\mu(\mathscr{S})$ be vector generating the flow from μ to s_i. By the definition of μ, the mean of v_i's is zero. Their covariance matrix $K \in \mathbb{R}^{m\times m}$ captures the second order variation of s_i's. Eigen decomposition of K provides the principal shape variations in the given collection. For instance, if V_i's are the principal eigenvectors of K, then $\psi_1(\mu,V_i)$'s provide the "eigen-shapes" of that family.

In the next section, we take a few specific examples of shape representations that have been used frequently in the literature.

3. APPROACHES TO SHAPE ANALYSIS

3.1 Landmark-Based Shape Analysis

The first formal mathematical theory of shapes is due to David Kendall [11] and is referred to as a Procrustes shape analysis. A remarkable body of work on analysis of shapes also exists due to works of Bookstein [3], Mardia [4], Small [15], and others. These studies share the property that objects (and their shapes) are represented using a finite number of landmarks (points in Euclidean spaces) and equivalences are established with respect to shape preserving transformations. Landmarks are chosen manually to capture shapes of objects in images. For instance, in medical images, landmarks may denote points of anatomical importance and are chosen by a medical expert. The resulting quotient space, a Riemannian manifold, is called the *shape space*.

The basic idea is to represent an object by k points, called *landmarks*; these points can be on boundary or inside the object which itself can be either two- or three-dimensional. This collection of points is an element of $\mathscr{C} = \mathbb{R}^{nk}$ where $n = 2$ or 3. To remove similarity transformations, consider the quotient space $\mathscr{S} = \mathbb{R}^{nk}/T$. Elements of $\mathscr{S}$ denote the shapes of interest, and an analysis of shapes becomes analysis of elements of $\mathscr{S}$. Translation and scaling transformations are easily removed from the representation by forcing the centroid to be zero, and by forcing the vector of coordinates to lie on a unit circle in $\mathbb{R}^{nk}$. For example, let $n = 2$, and equate $\mathscr{C}$ with $\mathbb{C}^k$ by considering the two coordinates of a landmark as real and imaginary parts of a complex number. Define $\mathscr{C}_1$ to be the subset of all zero-mean, unit complex vectors in $\mathscr{C}$; it is called a preshape space. From any observed shape $s \in \mathbb{C}^k$, remove its mean and scale using

$$s = s - \frac{1}{k}\sum_{i=1}^{k} s(i), \text{ and } s = s/\|s\| .$$

The resulting s is an element of the preshape space $\mathscr{C}_1$. However, the removal of rotation group is not straightforward and is performed as a minimization step. For any $s_1,\ s_2 \in \mathscr{C}_1$, define the rotational alignment as:

$$\hat{\theta} = \operatorname*{argmin}_{\theta\in\mathbb{S}^1} \|s_1 - \exp(j\theta)s_2\| . \quad (1)$$

Note that $\mathbb{S}^1$ acts as an isometry on the set $\mathbb{C}^k$. Defining $\hat{s}_2 = \hat{\theta}\cdot s_2$, a geodesic path between s_1 and $\hat{s}_2$ in $\mathscr{S}$ is given by $\psi_x(s_1,\hat{s}_2) = \cos(\alpha x)u_1 + \sin(\alpha x)u_2$, where

$$\alpha = \cos^{-1}(\langle s_1, \hat{s}_2\rangle),\ u_1 = s_1,\ u_2 = \frac{\hat{s}_2 - \langle \hat{s}_2, s_1\rangle}{\|\hat{s}_2 - \langle \hat{s}_2, s_1\rangle\|} . \quad (2)$$

It follows that $\alpha u_2 \in T_{s_1}(\mathscr{S})$ is the tangent direction such that $\psi_1(s_1;\alpha u_2) = s_2$.

Shown in Figures 4 and 5 is an example of this idea. Images shown in top panels of Figure 4 are used to extract landmarks shown in the bottom panels. These panels show the shape representations s_1 and $\hat{s}_2$ for the two objects present in top panels. Figure 5 shows the geodesic path between these two in $\mathscr{S}$. The landmarks have been connected by solid lines to improve display.

The Riemannian structure of $\mathscr{S}$ has been studied in several places including [13, 10]. The particularization of intrinsic means to this shape space was done in [14]. A brief

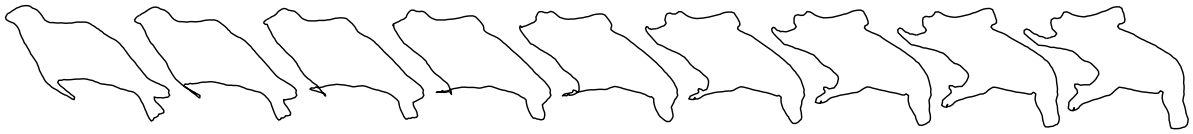

Figure 5: A geodesic path between the end shapes in landmark shape space. Landmarks have been connected by solid lines to improve display.

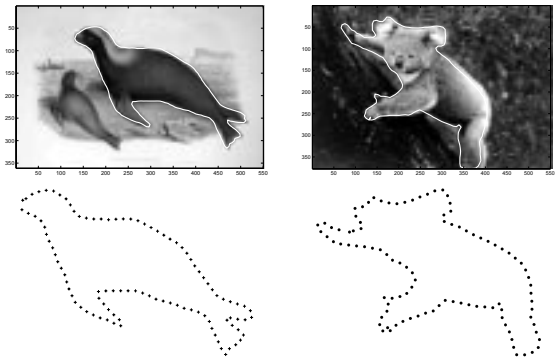

Figure 4: Landmark based shape analysis

summary follows: for a collection of shapes $s_1, s_2, \ldots, s_m$ in $\mathscr{S}$, let $y \in \mathscr{S}$ be an iterative estimate of the mean. Compute the generators of geodesic flows from y to s_i using the comment that follows Eqn. 2, and update according to Algorithm 1. Given the collection $s_1, s_2, \ldots, s_m$ in $\mathscr{S}$ and their mean μ, one can compute the covariance matrix $K \in \mathbb{C}^{k \times k}$ using the tangent vector $v_i \in \mathbb{C}^k$ that satisfy $\psi_1(\mu; v_i) = s_i$, $i = 1, 2, \ldots, m$. Dryden & Mardia [4] also describe procedures for testing hypotheses on $\mathscr{S}$ under some simple probability models.

An important strength of this approach is its computational efficiency and relative simplicity. These factors have contributed in development of advanced statistical analysis of shapes. In addition to means and covariances on shape spaces, researchers have derived techniques for shape testing, shape estimation, and shape extraction, all in statistical frameworks. Another strength is their applicability in any dimensions, $\mathbb{R}^2$, $\mathbb{R}^3$, or even $\mathbb{R}^n$ for large n. An important limitation of this approach is the need for pre-defined landmarks for analyzing shapes. In practice, it is difficult to extract landmarks automatically, and to register them across shapes, and this limits the scope of this approach.

3.2 Diffeomorphisms for Shape Matching

Another fundamental idea for shape analysis comes from Grenander's theory of patterns [5]. In this approach, the shapes are considered as points on an infinite-dimensional, differentiable manifold, and variations between shapes are modeled by actions of Lie groups on this manifold. Low-dimensional groups, such as rotation, translation and scaling, change the object instances keeping the shape fixed, while the high dimensional groups, such as diffeomorphism, smoothly change the object shapes ([17, 6]). This representation forms the mathematical basis of *deformable templates* as treated in [5, 1].

A brief introduction to this approach follows: Let $\mathscr{C}$ be the space of all images defined on a background space B; $\mathscr{C} = \mathbb{R}^B$. B is usually a unit square in $\mathbb{R}^2$ or a unit cube in $\mathbb{R}^3$. A space of shapes is given by $\mathscr{C}/T$, where T is the group of similarity transformations as earlier. Let $\mathscr{G}$ be the space of diffeomorphic maps from B to itself. Then, $\mathscr{G}$ forms a group action on $\mathscr{C}$ according to the map:

$$g \cdot I(x) = I(g \cdot x),\ g \in \mathscr{G},\ \ x \in B\ ,\ I \in \mathscr{C},$$

and $G \cdot I = \{g \cdot I : g \in \mathscr{G}\}$ defines the orbit of I under G. Note that G acts on $\mathscr{C}$ in an isometry, assuming the usual Euclidean metric on $\mathscr{C}$. Let ψ_x denote geodesic flows in $\mathscr{G}$ parameterized by x. The vector space $T_{id}(\mathscr{G})$, where id is the identity map from B to itself, is given by the set of smooth vector fields on B. The exponential map $\exp_{id} : T_{id}(\mathscr{G}) \mapsto \mathscr{G}$ is given by $\exp_{id}(v) = \psi_1(id; v)$.

A transformation between two images I_1 and I_2 can be modeled by diffeomorphically aligning I_1 to I_2. The resulting metric on the image space is given by:

$$d(I_1, I_2) = \operatorname*{argmin}_v \left(\lambda_1 \|I_2 - \exp_{id}(v) \cdot I_1\|_C^2 + \lambda_2 \|v\|_V^2\right)\ , \quad (3)$$

where $\|\cdot\|_C$ and $\|\cdot\|_V$ are generally chosen to be the Euclidean norm on the image space and the space of vector fields, respectively. The first term computes the smallest distance between the orbits of I_1 and I_2, while the second term measures the work done in aligning I_2 to I_1 via a diffeomorphism. The second term is equal to the length of geodesic from id to $\exp_{id}(v)$ in $\mathscr{G}$. λ_1 and λ_2 are simply the weights assigned to the two terms. This metric differs from the discussion in Section 2 in that the first term was always zero there, and only the second term, corresponding to geodesic lengths, played a role. Here, the pixel values in the image are included in the metric, while landmark-based shape analysis pixels values do not play any role.

Shapes here are considered implicitly through their full images. For example, to compare the shapes of boundaries of two 3D objects, one can embed each surface in a unit cube in $\mathbb{R}^3$ and seek the diffeomorphism that transforms one (3D) image into another. The distance between the two shapes is now given by Eqn. 3.

A computational simplification is obtained in Eqn. 3 when the term $\|I_1 - \exp(v) \cdot I_2\|$ is replaced by a function involving the landmarks in I_1 and I_2. Let X_1 be a set of landmarks in I_1 and X_2 be the corresponding set of landmarks in I_2. Then, $\|I_1 - I_2\|$ is replaced by $\|X_1 - X_2\|$ to obtain a speed up in computations. The speed comes from the fact that one needs to evaluate v only at the landmark locations and not on the whole B, as was the case earlier. However, this step requires a pre-defined and pre-registered set of landmarks on the two images. A strength of this approach is its applicability to shapes in $\mathbb{R}^n$ for arbitrary n. This can also take into

account the pixel values (or voxel values) while comparing shapes of two objects. However, the computational cost of finding the optimal match between two images is rather high.

3.3 Geometric Analysis of Shapes of Curves

There is an emerging family of techniques for studying the shapes of connected curves in Euclidean spaces. Both the geometry of curves and the geometry of spaces of curves play a role in this shape analysis. A brief introduction follows.

Let $\alpha : \mathbb{R} \mapsto \mathbb{R}^2$ denote the coordinate function of a curve parameterized by arc-length τ, i.e., satisfying $\|\dot{\alpha}(\tau)\| = 1$, for every τ. A direction function $s(\tau)$ is a function satisfying $\dot{\alpha}(\tau) = e^{js(\tau)}$, where $j = \sqrt{-1}$. s captures the angle made by the velocity vector with the horizontal axis, and is defined up to the addition of integer multiples of 2π. The curvature function $\kappa(\tau) = \dot{s}(\tau)$ can also be used to represent a curve.

Equivalence of shapes under similarity transformations is imposed as follows. Scaling is resolved by fixing the length of α to be 2π, and translations by representing curves via their direction functions. The rotation variability is removed by assuming that direction functions have a fixed average, say π. Thus, we consider the space $\mathbb{L}^2$ of all square integrable functions $s\colon [0,1] \mapsto \mathbb{R}$. $\mathscr{C}$ is the subspace of $\mathbb{L}^2$ consisting of all (direction) functions satisfying the constraints

$$\begin{aligned} \frac{1}{2\pi}\int_0^{2\pi} s(\tau)\,d\tau &= \pi; \int_0^{2\pi} \cos(s(\tau))\,d\tau = 0; \\ \int_0^{2\pi} \sin(s(\tau))\,d\tau &= 0. \end{aligned} \tag{4}$$

The last two equations ensure that a curve is closed. It is still possible to have multiple elements of $\mathscr{C}$ representing the same shape. This variability is due to the choice of the reference point ($\tau = 0$) along the curve. For $\theta \in \mathbb{S}^1$ and $s \in \mathscr{C}$, define $(\theta \cdot s)$ as a curve whose initial point ($\tau = 0$) is changed by a distance of θ along the curve. We term this a re-parametrization of the curve. To remove the variability due to this re-parametrization group, define the quotient space $\mathscr{S} \equiv \mathscr{C}/\mathbb{S}^1$ as the space of continuous, planar shapes. For details, please refer to the paper [12].

Next, we focus on the problem of finding a geodesic path between any two given shapes s_1, $s_2 \in \mathscr{C}$. The main issue is to find that appropriate direction $v \in T_{s_1}(\mathscr{C})$ such that a geodesic from s_1 in that direction passes through s_2 at time $x = 1$. In other words, the problem is to solve for a $v \in T_{s_1}(\mathscr{S})$ such that $\psi_0(s_1; v) = s_1$ and $\psi_1(s_1; v) = s_2$. One can treat the search for this direction as an optimization problem over the tangent space $T_{s_1}(\mathscr{C})$. The cost to be minimized is given by the functional $E(v) = \|\psi_1(s_1; v) - s_2\|^2$, and we are looking for that $v \in T_{s_1}(\mathscr{C})$ for which: (i) $E(v)$ is zero, and (ii) $\|v\|$ is minimum among all such tangents. Since the space $T_{s_1}(\mathscr{C})$ is infinite dimensional, this optimization is not straightforward. However, since $v \in \mathbb{L}^2$, it has a Fourier decomposition, and we can solve the optimization problem over a finite number of Fourier coefficients. For any two shapes $s_1, s_2 \in \mathscr{C}$, we have used a shooting method to find the optimal v [12]. The basic idea is to choose an initial direction v specified by its Fourier coefficients and then use a gradient search to minimize H as a function of the Fourier coefficients.

Shown in Figure 6 are two examples of geodesic paths in $\mathscr{C}$ connecting given shapes. Drawn in between are shapes corresponding to equally spaced points along the geodesic paths.

Statistical analysis of shapes using this representation is treated in the paper [12, 7].

4. CONCLUSION

In this paper we briefly introduce three different approaches to shapes analysis, and highlight their common aspects and their differences. A summary of comparisons is presented in Figure 7.

One approach that we have not covered here is the level set approach to image denoising, segmentation, and interpolation. Here, shapes are studied as level sets of a real-valued function defined on the image. Evolution of this function takes place according a partial differential equation (PDE) that is mostly driven two types of terms: one is data based where the driving force is dependent on the desired image pixels, and the second is a regularization term which penalizes the coarseness of this function. Different data terms and regularization terms lead to different properties of the resulting flow. Evolution of curves in this way has also been called *active contours* [9].

REFERENCES

[1] Y. Amit, U. Grenander, and M. Piccioni. Structural image restoration through deformable templates. *J. American Statistical Association*, 1991.

[2] R. Bhattacharya and V. Patrangenaru. Nonparametric estimation of location and dispersion on Riemannian manifolds. *Journal for Statistical Planning and Inference*, 108:23–36, 2002.

[3] F. L. Bookstein. Size and shape spaces for landmark data in two dimensions. *Statistical Science*, 1:181–242, 1986.

[4] I. L. Dryden and K. V. Mardia. *Statistical Shape Analysis*. John Wiley & Son, 1998.

[5] U. Grenander. *General Pattern Theory*. Oxford University Press, 1993.

[6] U. Grenander and M. I. Miller. Computational anatomy: An emerging discipline. *Quarterly of Applied Mathematics*, LVI(4):617–694, 1998.

[7] S. Joshi and A. Srivastava. A geometric approach to shape clustering and learning. In *Proc. of 12th IEEE Workshop on Statistical Signal Processing*, 2003.

[8] H. Karcher. Riemann center of mass and mollifier smoothing. *Communications on Pure and Applied Mathematics*, 30:509–541, 1977.

[9] M. Kass, A. Witkin, and D. Terzopoulos. Snakes: Active contour models. *International Journal of Computer Vision*, 1:321–331, 1988.

[10] D. G. Kendall, D. Barden, T. K. Carne, and H. Le. *Shape and shape theory*. Wiley, 1999.

[11] David G. Kendall. Shape manifolds, procrustean metrics and complex projective spaces. *Bulletin of London Mathematical Society*, 16:81–121, 1984.

[12] E. Klassen, A. Srivastava, W. Mio, and S. Joshi. Analysis of planar shapes using geodesic paths on shape spaces. *IEEE Pattern Analysis and Machiner Intelligence*, 26(3):to appear, March, 2004.

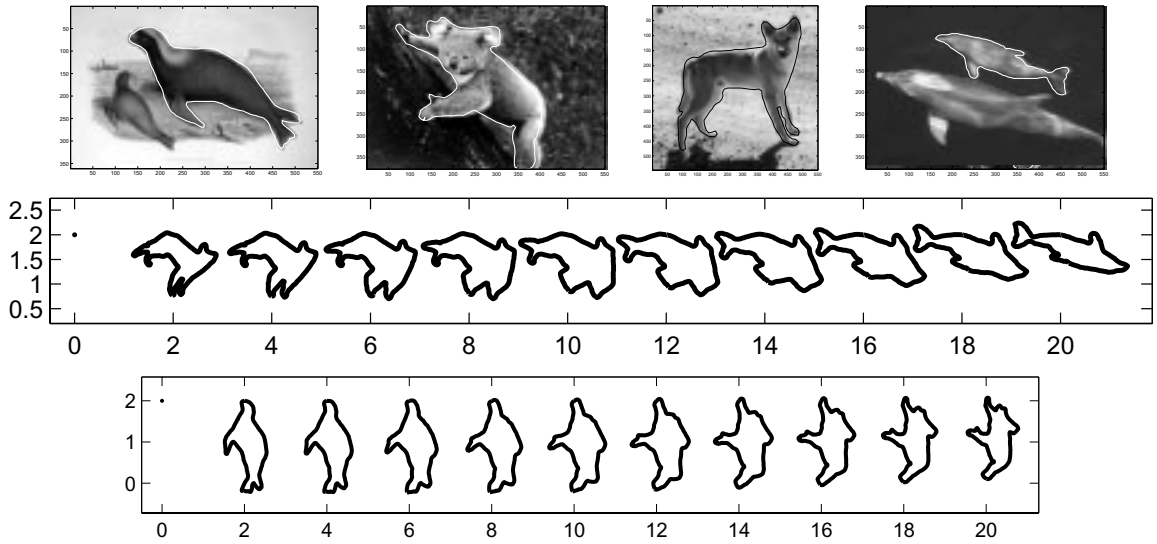

Figure 6: Top panels show examples of shapes manually extracted from the images. Bottom panels show examples of evolving one shape into another via a geodesic path. In each case, the leftmost shapes are s_1, rightmost curves are s_2, and intermediate shapes are equi-spaced points along the geodesic.

[13] H. Le. On geodesics in euclidean shape spaces. *J. Lond. Math. Soc.*, 44:360–372, 1991.

[14] H. Le. Locating frechet means with application to shape spaces. *Advances in Applied Probability*, 33(2):324–338, 2001.

[15] Christopher G. Small. *The Statistical Theory of Shape*. Springer, 1996.

[16] M. Steinberger. *Algebra*. PWS Publishing Company, Boston, 1994.

[17] A. Trouve. Diffemorphisms groups and pattern matching in image analysis. *International Journal of Computer Vision*, 28(3):213–221, 1998.

Aspects	Landmark Based	Diffeomorphism Based	Curve-Space Geometry
Representation ($\mathscr{C}$)	Location of landmarks $\mathbb{C}^k$	Full image $\mathbb{R}^B$, $B=[0,1]^2$	Direction functions of boundary curves in $\mathbb{L}^2(0,2\pi)$
Preshape $\mathscr{C}_1$	unit vectors with centroid zero	None	closed curves with average rotation π
Shape Space ($\mathscr{S}$)	$\mathscr{C}_1/\mathbb{S}^1$	$\mathscr{C}/T$	$\mathscr{C}_1/\mathbb{S}^1$
Extrinsic Group ($\mathscr{G}$)	None	Diffeomorphism on B	None
Geodesic Flow (ψ)	one-parameter flow on unit complex sphere	one-parameter flow on $\mathscr{G}$	one-parameter flow on $\mathscr{S}$
Tangent Vector ($v \in T_s(\mathscr{S})$)	Tangent to unit sphere	$v \in T_{id}(\mathscr{G})$, a vector field on B	a function normal to $\cos(s)$, $\sin(s)$
Metric	Geodesic Length on shape space	Geodesic Length on $\mathscr{G}$ plus a norm of Residual Image	Geodesic Length on shape space
Uses Pixel Values	No	Yes	No

Figure 7: A summary of different approaches to shape analysis. This table is particularized to shape analysis in $\mathbb{R}^2$.